Available online at www.sciencedirect.com

ScienceDirect

IFAC PapersOnLine 59-29 (2025) 150–155

Enhancing Magnetic Levitation Control via Moving Horizon Estimation: A Case Study on the Maggy System

Ørnulf Damsgaard * **Mikael Mjelde** * **Damiano Varagnolo** * **Hans Alvar Engmark** *

* *Department of Engineering Cybernetics, The Norwegian University of Science and Technology (NTNU). E-mail: ornulfd@stud.ntnu.no, mikael.mjelde@ntnu.no, damiano.varagnolo@ntnu.no, hans.a.engmark@ntnu.no*

Abstract: We consider how to improve the control of a magnetic levitation system by means of Moving Horizon Estimation algorithms. We thus derive such an online estimator, and analyse the improvements that it may bring to closed-loop state-feedback control performance. We explicitly consider a Moving Horizon Estimation (MHE) problem that accounts for linearized dynamical and measurement models, as long as actuation constraints, and for the purpose derive an unbounded quadratic programming formulation. Through experiments that involve LQR and Model Predictive Control (MPC) approaches we characterize the trade-offs among control performance and computation time, and characterize the robustness of the stabilization by investigating how estimation and control accuracy degrades under model inaccuracies. We discuss the effects of tuning on the results, how the estimation scheme may be improved, and how it may become advantageous especially for complex control maneuvers, full nonlinear models, and state/input bounds.

Keywords: Moving Horizon Estimation, state estimation, maglev control, LQR, MPC, Kalman filter

1. INTRODUCTION

Magnetic levitation (maglev) technology, widely recognized for applications such as high-speed trains and precision manufacturing, relies on active control to stabilize inherently unstable systems comprising levitating metallic objects thanks to opportunely controlled magnetic fields. Most academic research focuses on configurations where a magnetic object levitates beneath controlled electromagnets, and employs advanced strategies like feedback linearization, sliding mode control, or nonlinear model predictive control (NMPC). The complementary configuration where a permanent magnet hovers over a base of solenoids and fixed magnets has though received limited attention. This latter configuration, popular in small-scale displays, presents unique challenges in modeling and control, making it an ideal testbed for educational and research applications.

In this work we address the perceived gap by testing advanced estimation methods for such a maglev configuration. As a user case, we consider *Maggy*, a low-cost, modular maglev system designed for take-home labs that, unlike traditional maglev systems, employs a symmetric arrangement of solenoids and permanent magnets to levitate a magnet in 3D space (as in Fig. 1). More specifically, we consider a configuration that resembles planar magnetic motors used in high-precision industries (Wang et al., 2025). However, where characterizing and modelling such industrial systems often rely on computationally expensive finite element analysis (FEA, e.g., as in (Que and Lee, 2023)), in this paper we analyse how efficient semi-analytic models of magnetic fields and forces may enable real-time model predictive control through opportune receding horizon state observers.

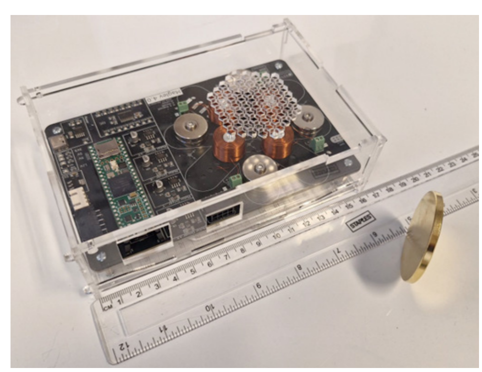

Fig. 1. The physical maglev setup considered in this paper. See the text below for details on parameters and conditions.

The scope of the paper is thus investigating how Moving Horizon Estimation (MHE) algorithms may enable state-feedback control of this type of maglevs, and which trade-offs lie behind these observer techniques.

Literature review: magnetic levitation has several applications, especially in high-speed trains (e.g., the Chuo

10.1016/j.ifacol.2025.12.197

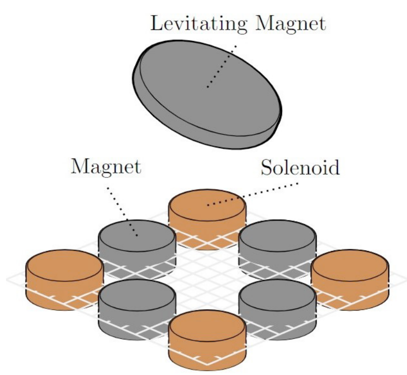

Fig. 2. The schematic representation of the magnetic part of the maglev setup considered in this paper.

Shinkansen (Uno, 2016)), protein analysis and disease diagnosis (Rahmani Dabbagh et al., 2021), and mechanical energy harvesting (Carneiro et al., 2020).

It has been shown by Engmark and Hoang (2023) that Maggy-like systems may be stabilized in practice using Proportional-Derivative (PD) controllers. At the same time, to the best of our knowledge we do not know whether the closed loop performance is constrained by the lack of full-state feedback. In other words, whether advanced strategies like Linear-Quadratic Regulators (LQR) or Model Predictive Controllers (MPC) may achieve better closed loop performance. To investigate this we propose and analyse what Moving Horizon Estimation (MHE) algorithms can bring to the table, i.e., analyse the benefits of building the estimation algorithm as a constrained optimization-based approach that leverages a dynamic model to reconstruct system states from noisy sensor data. It has been reported that MHE offers distinct advantages over Kalman filters, including explicit handling of nonlinearities and constraints, which are critical especially when a system is subject to highly coupled dynamics (Zhang et al., 2019).

MHE is though very relevant also in systems with slower dynamics, such as in industrial applications, and not just in fast real-time applications. Hedengren et al. (2007) for example shows how MHE can be implemented in an industrial gas phase polymerization reactor to estimate system states, parameters, and unmodeled disturbances. As an other example, Wang et al. (2014) shows an implementation of MHE in the power sector, specifically to achieve accurate dynamic power system state estimation.

MHE is then often linked with Model Predictive Control (MPC), and may be considered its dual. For example, Deniz et al. (2023) combines MHE and MPC for real-time control under bounded disturbances with a focus on robustness. Here the authors found a link between the horizon lengths of the MHE's backward horizon and the MPC's forward horizon and their connection to the system's closed-loop stability. Moreover, instead of relying on the MPC's terminal cost to serve as a Control Lyapunov Function (CLF) for closed-loop stability, as mentioned in Moreno-Mora et al. (2022), Deniz et al. (2023) finds a way to guarantee stability by choosing appropriate horizon lengths and cost function design.

Statement of contributions: this work aims at advancing magnetic levitation control by presenting and characterizing the first (to the best of our knowledge) implementation of a Moving Horizon Estimation (MHE) strategy for suspended maglev systems. We thus characterize what providing full-state feedback may enable, in terms of advanced control strategies like Linear-Quadratic Regulator (LQR) and Model Predictive Control (MPC), and investigate the sensitivity of the results from the MHE algorithm on its defining parameters (i.e., check how different tunings of the algorithm lead to different closed loop performance). We thus validate our approach through comprehensive simulations showing MHE's effectiveness, and use these for our analysis of the trade-offs between computational efficiency and estimation accuracy. For completeness, we actually consider just the problem of stabilizing the levitating magnet around one of its equilibria, and report that the best closed loop performance in stabilizing the Maggy system at equilibrium (with "best" in terms of the tradeoffs above) is obtained using a 15-step horizon.

Summarizing, the main contributions of this work are: (i) a high-fidelity yet computationally tractable model of a 3D magnetic levitation system, (ii) the integration of Moving Horizon Estimation (MHE) with Model Predictive Control (MPC) for robust stabilization, and (iii) a detailed analysis of estimation horizon trade-offs and robustness to model mismatch.

2. SYSTEM OVERVIEW

We consider a suspended magnetic levitation system to be primarily used for research and educational purposes. The system, shown in Fig. 1, prioritizes reconfigurability while maintaining portability. Unlike similar magnetic suspension systems such as the Magnetoshield (Takács et al., 2024), the considered setup operates as a multi-input multi-output (MIMO) levitation platform with flexible spatial configuration capabilities. This key distinction is immediately apparent in Fig. 3 and Fig. 1, which show the system's printed circuit board (PCB) and physical assembly respectively. The design incorporates a series of strategically placed mounting holes that enable various spatial arrangements of both electromagnets and permanent magnets. This feature intentionally introduces plant variability, supporting diverse control experiments within a single hardware platform with a compact footprint of $10 \times 15 \times 5$ cm when housed in its protective acrylic enclosure.

From a sensing and actuation point of view, Maggy is multi input multi output (MIMO), since comprising four electromagnetic coils as inputs, and nine Hall-effect sensors as outputs. The latter are strategically positioned for the detection of the position of the levitating magnet, and the system's software allows for flexible selection of sensor subsets, enabling experiments in sensor fusion and investigation of how estimation performance varies with different sensor configurations. (We note that the Hall-effect sensor array has been carefully positioned to minimize noise interference, though students are encouraged to explore additional filtering techniques as part of their control design exercises.) The actuation system, as said before consisting of four electromagnetic coils, actually integrate current sensing capabilities that facilitates actuator

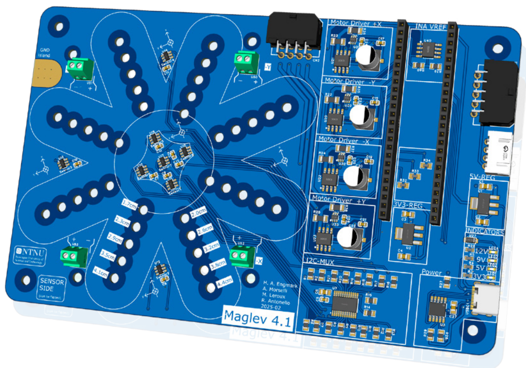

Fig. 3. A rendering of the PCB of the system. See text for details on parameters and conditions.

dynamics characterization. This feature provides valuable opportunities for students to study and compensate for real-world actuator non-idealities.

Computationally, the core of the system is a Teensy 4.1 microcontroller, selected for its balance between computational capability and affordability. Programmable in several languages, comprising C/C++, this platform delivers sufficient performance for real-time control implementations while remaining accessible to students with embedded systems experience.

Summarizing, the system intentionally preserves several real-world non-idealities, including actuator saturation and electromagnetic interference, and these characteristics provide authentic challenges to be addressed in the control and observer designs.

2.1 Mathematical modelling of the dynamics of the system

The electro-magnetic-mechanical dynamics of the considered magnetic levitation system may be accurately described (for the levitation control purposes) by a three-dimensional dynamic model whose complete state vector includes the position of the levitating magnet's center of gravity in Cartesian coordinates, the corresponding Euler rotation angles, and the translational and angular velocities. In the following we use this, as notation:

$$\boldsymbol{x}^T = [x, y, z, \alpha, \beta, \gamma, \dot{x}, \dot{y}, \dot{z}, \dot{\alpha}, \dot{\beta}, \dot{\gamma}] \tag{1}$$

The dynamic model can be derived from Newton-Euler equations where the forces and moments on the levitating magnet are calculated using the Biot–Savart law for the magnetic field and the Lorentz force law. Sending the interested reader back to Engmark and Hoang (2023) for more details, we here summarizes the main features of such a model. The forces can thus be described by means of

$$\boldsymbol{F} = \int_S \boldsymbol{K}(\alpha, \beta, \gamma) \times \boldsymbol{B}_{\text{base}}(x, y, z)\, dS \tag{2}$$

$$\boldsymbol{\tau} = \int_S \frac{1}{\mu_0} \boldsymbol{J}(\alpha, \beta, \gamma) \times \boldsymbol{B}_{\text{base}}(x, y, z)\, dS \tag{3}$$

where $\boldsymbol{K}$ represents the surface magnetization current and $\boldsymbol{J}$ the magnetic polarization.

The compact system can be expressed as

$$\dot{\boldsymbol{x}} = \boldsymbol{A}\boldsymbol{x} + \boldsymbol{B} f(\boldsymbol{x}, \boldsymbol{u}) \tag{4}$$

$$\boldsymbol{y} = \boldsymbol{C}\boldsymbol{x}. \tag{5}$$

For observability and controllability considerations, one may use a reduced-order model that does not include the states γ and $\dot{\gamma}$, resulting in a 10-dimensional state vector. The Hall sensors of the system measure then the magnetic field in the x, y, and z directions, providing a total of 9 three-dimensional measurements.

3. FUNDAMENTALS OF MOVING HORIZON ESTIMATION

Moving Horizon Estimation (MHE) provides a systematic approach for online state estimation by solving a constrained optimization problem over a receding time horizon. MHE can be thought as an opportune extension of advanced Kalman filtering, and provides a natural framework for handling nonlinear dynamics, measurement models, and state/input constraints. To the best of our understanding, MHE is particularly suitable for magnetic levitation systems, since physical limitations such as actuators saturation phenomena must be taken into account by the observer if one wishes to obtain state estimates that are accurate enough to be useful for closed loop control purposes.

In this paper we consider a MHE formulation that is based on a general discrete-time differential-algebraic equation (DAE) system model, i.e.,

$$\begin{aligned} \boldsymbol{x}_{k+1} &= F(\boldsymbol{x}_k, \boldsymbol{z}_k, \boldsymbol{u}_k, \boldsymbol{p}) + \boldsymbol{w}_k, \quad \boldsymbol{x}_0 = \boldsymbol{x}(t_0) \\ \boldsymbol{0} &= g(\boldsymbol{x}_k, \boldsymbol{z}_k, \boldsymbol{u}_k, \boldsymbol{p}) \\ \boldsymbol{y}_k &= h(\boldsymbol{x}_k, \boldsymbol{z}_k, \boldsymbol{p}) + \boldsymbol{v}_k \end{aligned} \tag{6}$$

where $\boldsymbol{x} \in \mathbb{R}^{n_x}$ represents the system states, $\boldsymbol{z} \in \mathbb{R}^{n_z}$ the algebraic states, $\boldsymbol{u} \in \mathbb{R}^{n_u}$ the control inputs, $\boldsymbol{p} \in \mathbb{R}^{n_p}$ unknown model parameters, and $\boldsymbol{y} \in \mathbb{R}^{n_y}$ the measurements. The terms $\boldsymbol{w}_k$ and $\boldsymbol{v}_k$ represent process and measurement noise, respectively.

Starting from the model above it is possible to then formulate a MHE optimization problem over a horizon of length N as

$$\begin{aligned} \min_{\boldsymbol{x}_{0:N}, \boldsymbol{z}_{0:N}, \boldsymbol{w}_{0:N-1}, \boldsymbol{p}} \quad & \left\| \begin{bmatrix} \boldsymbol{x}_0 - \bar{\boldsymbol{x}}_0 \\ \boldsymbol{p} - \bar{\boldsymbol{p}}_0 \end{bmatrix} \right\|^2_{\boldsymbol{P}_0} \\ & + \sum_{j=0}^{N} \|\boldsymbol{y}_j - h(\boldsymbol{x}_j, \boldsymbol{z}_j, \boldsymbol{p})\|^2_{\boldsymbol{R}_j} \\ & + \sum_{j=0}^{N-1} \|\boldsymbol{w}_j\|^2_{\boldsymbol{Q}} \end{aligned} \tag{7}$$

subject to the constraints

$$\begin{aligned} \boldsymbol{x}_{j+1} &= F(\boldsymbol{x}_j, \boldsymbol{z}_j, \boldsymbol{u}_j, \boldsymbol{p}) + \boldsymbol{w}_j, \quad j = 0, \ldots, N-1 \\ \boldsymbol{0} &= g(\boldsymbol{x}_j, \boldsymbol{z}_j, \boldsymbol{u}_j, \boldsymbol{p}), \quad j = 0, \ldots, N \\ \boldsymbol{x}_{j,\min} &\leq \boldsymbol{x}_j \leq \boldsymbol{x}_{j,\max}, \quad j = 0, \ldots, N \\ \boldsymbol{w}_{j,\min} &\leq \boldsymbol{w}_j \leq \boldsymbol{w}_{j,\max}, \quad j = 0, \ldots, N-1 \end{aligned} \tag{8}$$

The performance of MHE depends critically on a proper tuning of the weighting matrices $\boldsymbol{Q}$, $\boldsymbol{R}$, and $\boldsymbol{P}_0$. These matrices should ideally reflect the inverse covariances of the respective noise terms - the process noise $\boldsymbol{Q}$ determining, in other words, our trust in the dynamic model, while the measurement noise weight $\boldsymbol{R}$ reflecting confidence in sensor measurements.

Another factor that influences the performance of the MHE is the parameter N, the horizon length. As we investigate in the remainder of the paper, selecting different values for N means trading-off between estimation accuracy and computational complexity. For an embedded system like Maggy, the need is for achieving good estimation performance (and thus control performance) while maintaining real-time feasibility.

3.1 Formulating the MHE problem via linearized models

To save computational time at the cost of potential losses in the accuracy of the estimates, one may derive MHE implementations as quadratic programming (QP) problems with equality constraints if one assumes a linear(ized) model of the plant. Assuming process noise to account for deviations from the linearized model, and a classical LTI state space representation of the dynamics, the cost function for the MHE problem becomes

$$J = (\boldsymbol{x}_0 - \widehat{\boldsymbol{x}}_0)^T \boldsymbol{M} (\boldsymbol{x}_0 - \widehat{\boldsymbol{x}}_0) + \sum_{j=0}^{N-1} \boldsymbol{w}_j^T \boldsymbol{Q} \boldsymbol{w}_j + \sum_{j=0}^{N} \boldsymbol{v}_j^T \boldsymbol{R} \boldsymbol{v}_j \tag{9}$$

where $\boldsymbol{M}$, $\boldsymbol{Q}$, and $\boldsymbol{R}$ are positive definite weighting matrices for the arrival cost, process noise, and measurement noise, respectively.

The model constraints can then be formulated using a multiple shooting approach for a horizon of length N, i.e.,

$$\begin{aligned} \boldsymbol{x}_{j+1} - \boldsymbol{A}\boldsymbol{x}_j - \boldsymbol{w}_j &= \boldsymbol{B}\boldsymbol{u}_j \\ \boldsymbol{C}\boldsymbol{x}_j + \boldsymbol{v}_j &= \boldsymbol{y}_j. \end{aligned} \tag{10}$$

Unknown model parameters are not estimated directly but are accounted for by process noise. All decision variables can be collected in a vector $\boldsymbol{z}$ that includes the complete trajectories of the states $\boldsymbol{x}_{0:N}$, process noise $\boldsymbol{w}_{0:N-1}$, and measurement noise $\boldsymbol{v}_{0:N}$. The resulting QP problem has thus the form

$$\min_{\boldsymbol{z}} \frac{1}{2} \boldsymbol{z}^T \boldsymbol{G} \boldsymbol{z} + \boldsymbol{z}^T \boldsymbol{g} \quad \text{subject to} \quad \boldsymbol{A}_{\text{eq}} \boldsymbol{z} = \boldsymbol{b}_{\text{eq}} \tag{11}$$

and it can be using direct multiple shooting, where decision variables are estimated explicitly for each time step within the horizon. This approach can thus naturally handle constraints, but requires efficient quadratic programming solvers for real-time implementation.

3.2 Integrating MHE with MPC

The estimated states from MHE can be directly used by state-feedback techniques such as Linear Quadratic Regulators (LQR) or Model Predictive Control (MPC) schemes - implementing thus a classical observer-controller separation approach.

4. EXPERIMENTAL RESULTS AND ANALYSIS

The implementation and evaluation of the linear MHE approach for the magnetic levitation system under consideration was conducted through four different types of simulation experiments, each designed to assess different aspects of the estimator's performance and practical applicability.

4.1 Determining a Suitable Horizon Length

The first experiment investigated the trade-off between estimation accuracy and computational burden by varying the MHE horizon length N from 4 to 30 steps.Using Monte Carlo simulations with 5 runs per configuration, the Root Mean Square Error (Root Mean Square Error (RMSE)) was evaluated across all system states. The results confirm intuitions, and thus show a clear inverse relationship between horizon length and estimation error, with total RMSE decreasing asymptotically as N increased. However, computational runtime increased proportionally, creating a practical optimization problem.

The analysis (cf. Fig. 4 and Fig. 5) revealed that a horizon length of $N = 15$ provided an suitable balance, yielding minimal RMSE spread ($\pm 1\sigma$) while maintaining acceptable computational performance. State-specific analysis showed heterogeneous behavior: position states (x, y), orientation states (α, $\dot{\alpha}$, $\dot{\beta}$) benefited significantly from longer horizons, while velocity estimates ($\dot{x}$, $\dot{z}$) showed degraded performance with increasing N. This phenomenon suggests that the linearized model's accuracy varies across different state variables, with position and orientation dynamics being better captured than velocity dynamics.

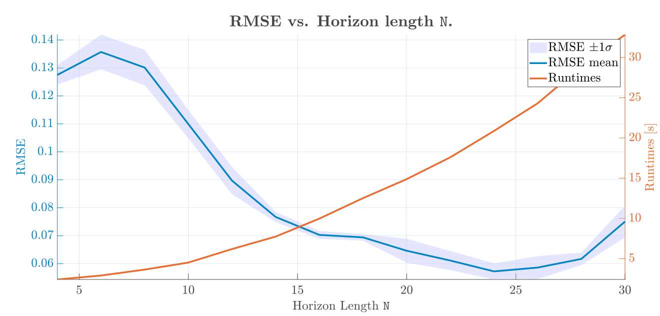

Fig. 4. Total RMSE and average runtimes versus horizon length. Runtimes were measured in MATLAB R2024b on a machine with an AMD Ryzen 9 7950X3D @ 5.5 GHz and 64 GB RAM.

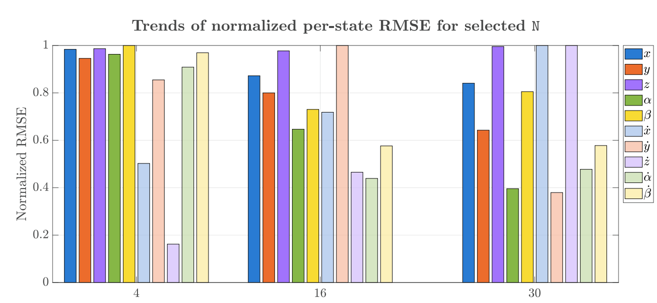

Fig. 5. Normalized per-state RMSE for a selection of horizon lengths. See the text below for details on parameters and conditions.

4.2 Closed-Loop Control Performance

The second experiment evaluated MHE-based closed-loop control in simulation, comparing ground-truth (GT) and MHE-estimated state feedback. The system employed a dual-controller architecture: Linear Quadratic Regulator (LQR) for initial stabilization, switching to Model Predictive Control (MPC) when the Normalized Innovation Squared (NIS) remained within 95% confidence bounds.

MHE state estimates exhibited initial transients before converging to track the ground-truth states effectively. The estimator demonstrated robust measurement tracking and smoothing across all three magnetic sensors, with position and orientation estimates showing particularly good fidelity. Control switching occurred at approximately 0.18 seconds, when estimation confidence reached acceptable levels as indicated by NIS statistics.

Comparison between GT and MHE-based simulations revealed significant initial trajectory deviations, but both systems ultimately achieved stable levitation at the desired equilibrium. The MHE-based control inputs showed more symmetric behavior between positive and negative solenoids, suggesting that estimation noise influenced the control strategy while maintaining overall system stability.

4.3 Robustness Under Model Mismatch

The third experiment assessed MHE performance under deliberate model uncertainties, simulating real-world conditions where the estimator's internal model differs from the actual system. Model parameters were adjusted to emulate a heavier levitating magnet (0.08 kg vs. 0.07 kg), larger radius (0.022 m vs. 0.02 m), and 1 mm misalignment of base magnets. Process noise weights were reduced by an order of magnitude (10^6 to 10^5) to accommodate increased model uncertainty.

Despite these mismatches, position and orientation estimates maintained convergence behavior similar to the nominal case, demonstrating inherent robustness. However, translational velocity estimates exhibited sharp initial spikes, and angular velocities converged more slowly, indicating sensitivity to model accuracy in derivative states. The NIS trajectory required longer to stabilize (0.2 seconds vs. 0.18 seconds), and temporarily exceeded bounds around 0.6 seconds, triggering brief LQR reactivation.

Innovation analysis using the Ljung-Box test revealed mild autocorrelation in measurement residuals, suggesting (as it should be) suboptimal tuning under model mismatch conditions. This highlights the critical importance of proper weight matrix selection when model uncertainties are present.

4.4 Hardware Validation and Computational Analysis

The final experiment validated both MHE and Kalman Filter (KF) performance using real sensor data from the physical magnetic levitation system. Both estimators were initialized with equivalent weight matrices (MHE weights and inverse KF covariances) to ensure fair comparison.

Real-data validation revealed a convergence period of approximately 2 seconds, corresponding to the physical placement of the levitating magnet. Both estimators achieved similar steady-state performance, with MHE showing marginally better transient tracking during initial convergence. However, computational analysis revealed stark differences in execution time: the Kalman filter required 0.0517 ms per iteration, while MHE demanded 4.40 ms ($N = 3$) to 28.3 ms ($N = 15$) per iteration—representing a 85× to 547× computational overhead.

The measurement tracking analysis showed both estimators provided effective noise smoothing compared to raw sensor data, with occasional steady-state offsets that were consistent between methods. Reducing the MHE horizon to $N = 3$ produced minimal performance degradation while significantly improving computational efficiency, though still remaining an order of magnitude slower than the Kalman filter.

5. CONCLUSIONS AND RECOMMENDATIONS

This study investigated moving horizon estimation (MHE) as a state estimation and filtering strategy for maglev systems with levitation above the actuator plane. An horizon length of 15 steps emerged as a practical balance between estimation accuracy and computational efficiency for this specific platform, though experimental limitations left some aspects inconclusive. Simulations confirmed that MHE enables stabilization via LQR/MPC despite transient deviations and exhibits resilience to model mismatch, albeit with increased initial errors in translational velocity. While MHE and the Kalman filter yielded comparable estimation performance for equilibrium stabilization, MHE's computational overhead posed significant challenges for real-time implementation, favoring the Kalman filter in linearized scenarios. Nevertheless, MHE's constraint-handling capabilities and potential compatibility with nonlinear models suggest untapped advantages for future applications involving complex maneuvers, full nonlinear dynamics, or explicit constraints. Shorter horizons may further optimize computational efficiency for real-time use. Though the study validated MHE-based control in simulation, physical implementation and refinement of robustness tuning—particularly through weight matrix optimization—remain critical for practical deployment. Finally, we remark that these findings highlight a trade-off: while MHE's advanced features are theoretically promising, its current limitations necessitate careful consideration of problem-specific requirements before adoption.

REFERENCES

Carneiro, P., Soares dos Santos, M.P., Rodrigues, A., Ferreira, J.A., Simões, J.A., Marques, A.T., and Kholkin, A.L. (2020). Electromagnetic energy harvesting using magnetic levitation architectures: A review. *Applied Energy*, 260, 114191.

Deniz, N., Sanchez, G., Murillo, M., and Giovanini, L. (2023). Simultaneous moving horizon estimation and control for nonlinear systems subject to bounded disturbances. *Int. J. Robust Nonlinear Control*, 33. doi: 10.1002/rnc.6799.

Engmark, H.A. and Hoang, K.T. (2023). Modeling and control of a magnetic levitation platform. *IFAC-PapersOnLine*, 56(2), 7276–7281.

Hedengren, J., Allsford, K., and Ramlal, J. (2007). Moving horizon estimation and control for an industrial gas phase polymerization reactor. In *Proc. Amer. Control Conf. (ACC)*, volume 7, 1353–1358. doi: 10.1109/ACC.2007.4282820.

Moreno-Mora, F., Beckenbach, L., and Streif, S. (2022). Predictive control with learning-based terminal costs using approximate value iteration. ArXiv preprint arXiv:2212.00361.

Que, Z. and Lee, K.M. (2023). Analytical design methodology based on distributed current source models for parametric study of a three-dof planar motor. *2023 IEEE/ASME International Conference on Advanced Intelligent Mechatronics (AIM)*, 543–548. doi: 10.1109/AIM46323.2023.10196159.

Rahmani Dabbagh, S., Alseed, M.M., Saadat, M., Sitti, M., and Tasoglu, S. (2021). Biomedical applications of magnetic levitation. *Advanced NanoBiomed Research*, 2, 2100103.

Takács, G., Mihalík, J., Gulan, M., Vargová, A., Mikuláš, E., and Ožana, Š. (2024). Magnetoshield: A novel open-source magnetic levitation benchmark device for mechatronics education and research. *Sensors*, 24(2).

Uno, M. (2016). Chuo shinkansen project using superconducting maglev system. *Japan Railway & Transport Review*, 68, 14–25.

Wang, G., Kim, S.J., and Giannakis, G.B. (2014). Moving-horizon dynamic power system state estimation using semidefinite relaxation. In *IEEE Int. Conf. Acoust., Speech Signal Process. (ICASSP)*, 3963–3967. doi: 10.1109/ICASSP.2014.6854291.

Wang, R., Zhang, L., Shi, C., Zhao, C., and Yang, K. (2025). Analysis and optimization of a moving magnet permanent magnet synchronous planar motor with split halbach arrays. *Energies*. doi:10.3390/en18061388.

Zhang, W., Wang, Z., Zou, C., Drugge, L., and Nybacka, M. (2019). Advanced vehicle state monitoring: Evaluating moving horizon estimators and unscented kalman filter. *IEEE transactions on vehicular technology*, 68(6), 5430–5442.